Exchange Constants and Knight-Shift Anisotropy in Single-Crystal Lead†

J. Schratter* and D. Llewelyn Williams
Physics Department, University of British Columbia, Vancouver 8, British Columbia, Canada
(Received 6 July 1971)

Nuclear-magnetic-resonance studies of the angular dependence of the resonance frequency, the linewidth, and the second moment have been made upon a lead single crystal. The "exchange-narrowing" model has been shown to be inapplicable to lead. The angular variation of the second moment has established that the contribution from the second-nearest neighbors is very small and values are obtained for the pseudoexchange and pseudodipolar coefficients for the first-nearest neighbor of $J_1 = 4.64$ kHz and $b_1 = 1.75$ kHz, in moderate agreement with the theoretical values of Tterlikkis, Mahanti, and Das of $J_1 = 4.81$ kHz and $b_1 = 1.48$ kHz. A small anisotropy of the Knight shift which has the expected angular dependence has been observed for the first time in a cubic metal.

I. INTRODUCTION

The NMR linewidth in heavy metals is substantially larger than the width calculated from the dipolar interaction alone.[1] The main contributions responsible for this increase are the pseudoexchange[2] and pseudodipolar[3] interactions. The former is of scalar nature and produces the so-called exchange narrowing in the case of like spins and broadening for unlike spins. The latter has the same tensorial form and symmetry as the dipolar interaction and always broadens the line.

Van Vleck[1] has shown that the second moment of the absorption line in substances containing only one magnetic isotope is not affected by the pseudoexchange interaction. This makes it possible to separate out the pseudodipolar contribution in a second-moment measurement. Lead is a suitable metal for this type of investigation since it contains only one magnetic isotope (21% abundance), and, moreover, is of spin $I = \frac{1}{2}$, thus escaping the additional difficulties which might arise from quadrupolar interactions.

Previous experimental work on the linewidth mechanisms in lead[4-6] was done on powdered samples and under the assumption that the NMR line obeys the Anderson-Weiss model[7] of extreme exchange narrowing. The justification for this assumption came from the fact that the NMR line in lead had a cutoff Lorentzian shape, as predicted by this theory. In this case the linewidth is proportional to the second moment divided by the rate of exchange.[7,8] Thus one can obtain information about the pertinent interactions by measuring linewidths instead of the experimentally more difficult second moments.

In this work we studied a lead single crystal in order to directly observe the angular dependence of the second moment and thus obtain additional information not obtainable from powder results. It was initially intended to tackle this problem following the method of Sharma, Williams, and Schone[9] in their study of white tin, where it was found that the angular dependence of the linewidth had the form expected for that of the second moment. This was taken as evidence for the proportionality between the second moment and the linewidth predicted by the Anderson-Weiss model, and the coupling constants were then largely determined from the linewidths. However, we find that the linewidth in the case of lead does not exhibit the expected angular dependence characteristic of the second moment, although the lines are Lorentzian in the center, and we are thus forced to attempt direct determinations of the second moments. Definite conclusions are presented regarding the radial dependence of the exchange constants and the values are compared with the previous experimental results and the theoretical calculation recently made by Tterlikkis, Mahanti, and Das.[10]

The fractional difference in resonance frequency between metal and reference compound, called the Knight shift,[11] depends in general on the direction of the applied magnetic field with respect to the crystalline axes.[12] One commonly writes $\Delta\vec{H} = \underline{K}\vec{H}$, where $\underline{K}$ is a second-rank tensor. The isotropic part of the shift, given by $K_{iso} = \frac{1}{3}\mathrm{Tr}\{\underline{K}\}$, has been studied extensively, mainly in powder samples which are perfectly adequate for this type of work. The anisotropic shift has been investigated in metals of symmetry lower than cubic using both powder and single-crystal samples.

If the anisotropic contribution is large the powder samples may prove adequate enough; however, single-crystal samples become of paramount importance when accurate measurements are required.

Using group-theoretical arguments Boon[13] has shown that in the absence of spin-orbit coupling the anisotropic Knight shift in cubic metals is identically zero. A small anisotropic contribution is expected in the case of strong spin-orbit coupling.

No such effect has been seen prior to this work.

Lead is again a choice candidate for a search for this effect since it is a heavy cubic metal with a large Knight shift and a relatively small linewidth. We have therefore carefully studied the angular variation of the resonance frequency of our resonance lines and we find a small anisotropic contribution to the Knight shift which is consistent with the expected angular dependence.

II. EXPERIMENTAL METHOD

The signals were observed with a Pound-Knight spectrometer whose frequency was swept with a varicap PC116 mounted in the tank circuit. The magnetic field, kept constant at 9.5 kG, was produced by a rotatable 12-in. Varian magnet and was monitored continuously by a glycerine probe situated near the sample. In a typical measurement, the field did not vary by more than 30 mG during the time taken to record a resonance line. However, corrections were made for variations of more than 15 mG. The absolute value of the field measurement was of little importance since we were not interested in establishing the isotropic Knight shift to very high accuracy. However, our field measurement had to be invariant with respect to rotations of the magnet. To check this, we placed a deuteron probe at the site of the lead sample and measured the ratio between its resonance frequency and that of the field monitor probe as a function of angle. This ratio was found to be constant within 1 part in 10^6, which corresponds to 10 mG and is therefore perfectly adequate for our measurements. The homogeneity over the specimen volume was of the order of 3 parts in 10^6. A set of Helmholtz coils mounted on the pole faces provided the modulation field needed for phase-sensitive detection. The modulation frequency was 38 Hz. The crystal specimen, supplied by Metals Research Ltd., was of 99.99% purity, cylindrical in shape (12-mm diam $\times$ 25 mm in length), and had the cylinder axis along the [110] orientation. It was mounted with this axis perpendicular to the magnetic field such that, by rotating the magnet, one swept the dc field in the plane containing the [001], [$\bar{1}$11], and [$\bar{1}$10] axes.

It was found that the orientation of the crystal could be determined accurately by recording the magnetoresistance signal at liquid-helium temperatures. The latter plays the role of a strong but constant base-line shift for a given orientation, but is strongly orientation dependent. For instance, it has a sharp extremum when the field is along the [$\bar{1}$11] axis.

The measurements were made at 1.2 K by pumping on liquid helium. At this temperature the T_1 contribution to the linewidth is negligible.

III. RESULTS

The experimental line in a bulk-metallic specimen is a mixture of absorption and dispersion modes as a result of the variation in the phase of the radio-frequency field with depth of penetration into the metal. [14] The small skin depth reduces the effective sample volume to a thin outer layer of the specimen, but with a sensitive spectrometer one can obtain reasonable signal-to-noise ratios. One of the better signals obtained with a modulation low compared to the linewidth is shown in Fig. 1. We have analyzed the lines to obtain resonance frequencies and linewidths by fitting a set of modulated mixtures of absorption and dispersion modes of Lorentzian lines using the formalism developed by Wahlquist. [15] The fits are satisfactory for modulation amplitudes up to about 30% of the linewidth (defined as the width at half-intensity of the absorption mode), and suggest that the lines are of Lorentzian shape over regions up to two linewidths from the resonance frequency. It is not possible to fit the lines with a Gaussian profile. However, the behavior of the line at large modulation amplitudes is not understood. No lines of modulation amplitude larger than 25% of the linewidth were used for the data presented throughout this work.

The modulated mixed mode of a Lorentzian line at the output of a lock-in amplifier of infinitely short time constant is of the form

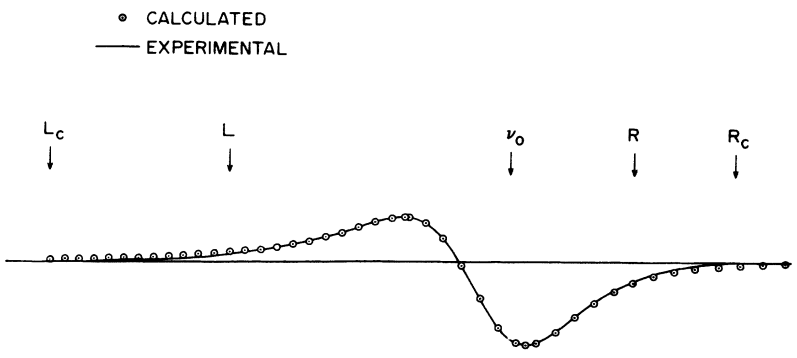

FIG. 1. Fitted experimental line. The symbols are explained in the text. It should be noted that the figure represents a reduction of 1:6 of the data, which masks the clarity of the cutoff points.

$$\chi = \chi'' + C\chi = A \int_{-\tau}^{\tau} \frac{[W - C(H_d + h_m \cos t)] \cos t \, dt}{W^2 + (H_d + h_m \cos t)^2} \quad , \tag{1}$$

where the line shape χ depends on the mixture of the modes C, the half-width at half-intensity of the absorption mode W, and the modulation amplitude h_m, but does not depend on the modulation frequency. W is a normalizing constant, and $H_d = H_a - H_0$, where H_a is the sweeping field and H_0 the resonance field. A point-by-point representation of the line shape given by Eq. (1) was obtained by computer. Each point was then corrected for time-constant effects by computing the expression

$$y(t) = \frac{1}{RC} \int_0^t \chi(t') \exp\left(-\frac{t' - t}{RC}\right) dt' \, ,$$

where RC is the time constant of the lock-in amplifier. We felt that these corrections were necessary since our lines are asymmetric and the linewidths anisotropic in character. The calculated line shapes fitted our experimental results very well. It is worthwhile mentioning that the quality of the fitting shown in Fig. 1 is characteristic of all other lines as well.

The sample was chosen of low purity to prevent any possible de Haas–van Alphen oscillation effects. A preliminary experiment to check for these oscillations as well as to get an idea of our accuracy was performed at 1.2 K. We determined the position of the larger peak of the derivative of the resonance line for different field values and small variations in ψ around 0° (the angle is measured between the direction of the field and the [001] axis). The root-mean-square deviation of the peak position for nine lines was 24 Hz in 9 MHz.

The angular dependence of the linewidth is shown in Fig. 2. It has been shown by O'Reilly and Tsang[16] that the most general allowed angular dependence of the second moment (M_2) for a cubic crystal, assuming interactions of dipolar symmetry, is of the form

$$M_2 = P(x^4 + y^4 + z^4 - Q) \, , \tag{2}$$

where P and Q are two independent parameters and x, y, z are the direction cosines specifying the orientation of the magnetic field with respect to the crystallographic axes. It will be immediately noted from Fig. 2 that the angular variation of the linewidth is not in accordance with this dependence, in contrast to the white-tin results. We are therefore forced to attempt a direct determination of the orientation dependence of the second moment. This is indeed difficult since the resonance lines are Lorentzian for the central region and the signal-to-noise ratio is poor in the wings.

The second moment is defined as

$$M_2 = \int_{-\infty}^{+\infty} x^2 \chi''(\omega) \, dx \int_{-\infty}^{+\infty} \chi''(\omega) \, dx \, ,$$

where $x = \omega - \omega_0$, i.e., the deviation of the frequency from the resonance frequency ω_0. We may note that if the observed line is a mixture of modes, i.e., $\chi = a\chi''(\omega) + b\chi'(\omega)$, this relation may be written replacing χ'' by χ without affecting the result since $\chi'(\omega)$ is an odd function of x. Of course, errors in the resonance frequency, determined from the previous curve fitting, will introduce some error, but this is a very small effect. The second moment may also be defined in terms of the derivatives of the resonance line:

$$M_2 = \left(\frac{1}{3} \int_{-\infty}^{+\infty} x^3 \frac{d}{dx} \chi(\omega) \, dx\right) \Big/ \left(\int_{-\infty}^{+\infty} x \frac{d}{dx} \chi(\omega) \, dx\right) .$$

The second-moment calculations were made using this expression and making the following approximation to the experimental line in view of the weak signals in the wings. The computer was fed the following parameters of the experimental line as illustrated in Fig. 1; W, h_m, C, as defined above, the resonance frequency ν_0, the left- and right-hand-side points at which the line begins to deviate from the Lorentzian fit (L and R), and the two cut-off points L_c and R_c determined by a linear extrapolation to the base line. When the shape of the

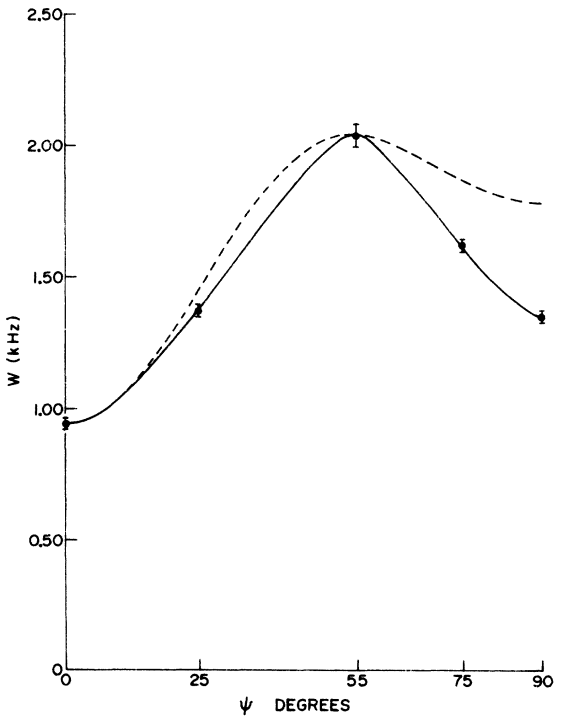

FIG. 2. Angular dependence of the linewidth W. ψ is the angle between the [001] crystallographic axis and the direction of the magnetic field in the (110) plane. The error bars represent the root-mean-square deviations of the experimental results. The dashed curve represents the predicted angular variation of the second moment.

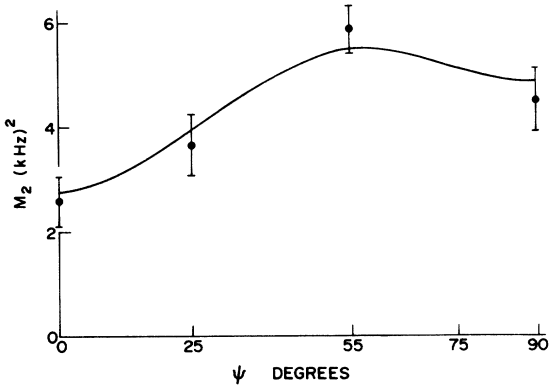

FIG. 3. Angular dependence of the second moment. The error bars represent the root-mean-square deviations of the experimental results and the solid line is the best fit in keeping with the allowed angular dependence.

line showed nonlinear cutoffs, the tail contribution was calculated manually. The computer determined the total second moment and also the different contributions to M_2 from different parts of the line. It turns out that the dominant factor is L_c (since on the left side of the line the absorption and dispersion contributions add) and the other parameters are of much less importance. One may argue that ν_0 and L_c must have the same influence on M_2, since their difference enters the computation. However, in practice the error in determining ν_0 is much less than that in determining L_c, and in this sense L_c is the determining factor. This result is indeed fortunate since R_c, the right-hand cutoff, is hard to determine. The second moments were then corrected for modulation by subtracting $\frac{1}{4}h_m^2$ according to the result of Andrew.[17] The results are shown in Fig. 3. It will be seen that there is some scatter in the results, but a definite pattern emerges which allows definite conclusions to be drawn as will be shown in Sec. IV.

The experimental Knight-shift results are shown in Fig. 4. The smooth curve represents the best fit for the expected angular dependence: It yields for the resonance frequency

$$\nu_0 = 9004.41 + 0.285\ (\tfrac{1}{2}\sin^4\psi + \cos^4\psi - 0.6)\ \text{kHz}.$$

From Fig. 2 we see that the linewidth at $\psi = 25°$ is approximately the same as that at $\psi = 90°$, and the fact that we obtain reasonable differences in the resonance frequencies at these two orientations is an indication that the anisotropy of the Knight shift is not due to fitting errors introduced by the anisotropy of the linewidth.

IV. DISCUSSION

A. Exchange Constants

The second moment of a single-crystal line, containing only one magnetic isotope, is given by[1]

$$M_2 = \tfrac{3}{4}\gamma^4\hbar^2 I(I+1) f \sum_k (1+B_k)^2 \left(\frac{(1-3\cos^2\theta_k')^2}{R_k^6}\right), \tag{3}$$

where it is assumed that all crystal sites are equivalent, and the sum is calculated with respect to one site chosen as the origin. R_k is the distance of nucleus k from the origin, θ_k' is the angle between $\vec{R}_k$ and $\vec{H}$, γ is the nucleus-gyromagnetic ratio, f is the abundance of the magnetic isotope, and $B_k = R_k^3 b_{ik}/\gamma^2\hbar$, where b_{ik} is the pseudodipolar coupling constant defined by[3]

$$H_{ij}^{\text{pd}} = b_{ij}\left((\vec{I}_i\cdot\vec{I}_j) - \frac{3(\vec{I}_i\cdot\vec{R}_{ij})(\vec{I}_j\cdot\vec{R}_{ij})}{R_{ij}^2}\right),$$

where H_{ij}^{pd} is the pseudodipolar interaction between spin I_i and spin I_j (joined by $\vec{R}_{ij}$) via the conduction electrons. A fairly complicated theoretical expression for b_{ij} was given by Bloembergen and Rowland in their original paper,[3] and more recently by Tterlikkis, Mahanti, and Das,[18] who made a relativistic second-order perturbation calculation, using Dirac-orthogonalized-plane-wave functions. As far as we know, the only theoretical calculation of b_{ij} for the case of lead has been attempted by the same authors[10] using the formalism developed in Ref. 18. Even though they have used some of the details of the lead Fermi surface, which has been extensively investigated with de Haas–van Alphen oscillation techniques by Anderson and Gold,[19] their calculation essentially provides an isotropic result for the coupling constant b_{ij}, as has been the case with all theoretical calculations of b_{ij} in metals to date. In real metals, however, it is known[3,18] that b_{ij} does depend on the orientation of the position vector joining the two nuclei. Measurements on powders

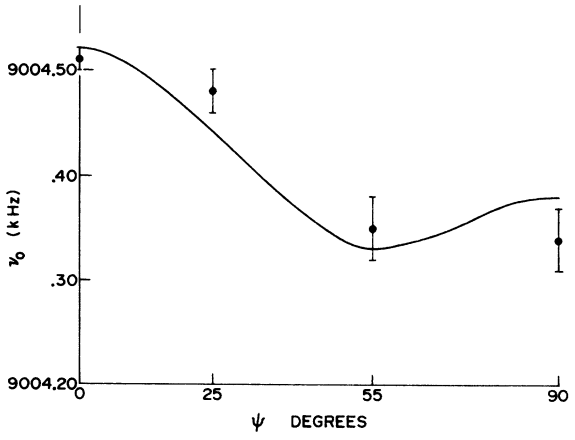

FIG. 4. Angular dependence of the resonance frequency. The error bars represent the root-mean-square deviations of the experimental results and the solid line is the best fit in keeping with the allowed angular dependence.

cannot establish this orientation dependence. We hope that work on single crystals will stimulate calculations that take this anisotropy into account.

The oscillatory character of the radial dependence of b_{ij}, as well as the above-mentioned anisotropy, makes it often difficult to choose the shells which have the major contribution to the second moment of the line. If, for example, $b_{ij}(R_{ij})$ happens to have a zero at the nearest-neighbor distance, then it is the shell formed by the next-nearest neighbors which gives the major contribution to the linewidth. Since different shells belong, in general, to different symmetries, it is again the work on single-crystal samples that can help decide upon this point. Alloul *et at.*[5,6] have used the spin-echo technique on powdered samples to determine the coupling constants b_{ij} and J_{ij}. The spin-echo measurement furnishes for each shell k a modulation frequency given in first approximation by

$$\nu_k = \frac{1}{2\tau_m} = \frac{1}{4\pi}\left(J_k + \frac{\gamma^2\hbar}{R_k^3}(1+B_k)\right) , \tag{4}$$

where $2\tau_m$ is the period of the modulation and J_k is the coupling constant of the pseudoexchange interaction. In order to determine J_k and B_k independently, the spin-echo data must be combined with cw data on second moments. Since the latter were experimentally difficult to obtain, Alloul *et al.* used the Anderson-Weiss model which predicts[20]

$$W = \frac{2.36 f^{\frac{1}{2}}}{2\pi}\ \frac{(\gamma^2\hbar/R_{01}^3 + b_{01})^2}{J_1} , \tag{5}$$

where only the first-nearest-neighbor interaction has been taken into account. The experimental echo envelopes showed only one clearly defined modulation period,[5] $2\tau_m = 305 \pm 15$ μsec. It was not clear whether it was produced by the first- or second-nearest neighbors. The experimental half-linewidth was $W = 1.22 \pm 0.04$ kHz. Using these data and the relations (3) and (4), they obtained two sets of data for the coupling constants, corresponding to the two possible choices in which ν_k is attributed to either the first or second shell of neighbors, respectively.

O'Reilly and Tsang[16] have shown that two independent parameters are required to specify the most general allowed angular variation of the second moment in cubic-crystal structures. In the case of lead, which has a fcc structure, this dependence is of the form given by Eq. (2). Equation (3) can be written in the form[16]

$$M_2 = \frac{12\pi}{5}\gamma^4\hbar^2 I(I+1) f \sum_k \frac{(1+B_k)^2\, Y_2^0(\theta_k', \phi_k')\, Y_2^0(\theta_k' \phi_k')}{R_k^6}$$

$$= \frac{12\pi}{5}\gamma^4\hbar^2 I(I+1) f \sum_k \frac{(1+B_k)^2}{R_k^6}\left[X_0^1(\theta_k, \phi_k)\, X_0^1(\theta, \phi) + \tfrac{2}{7} X_4^1(\theta_k, \phi_k)\, X_4^1(\theta, \phi)\right] ,$$

where X_i^μ are lattice harmonics of the crystal,[16] (θ_k, ϕ_k) are the spherical angles made by $\vec{R}_k$, and (θ, ϕ) are those made by $\vec{H}$ with the crystallographic axes. Using the appropriate expressions for the lattice harmonics, we finally obtain

$$M_2 = \tfrac{3}{5}\gamma^4\hbar^2 I(I+1) f \sum_k (1+B_k)^2 S_k ,$$
$$S_k = \frac{1}{4R_k^6}\left[37.5\,(\sigma_k - 0.6)\sigma - 2.5\sigma_k + 17.5\right] , \tag{6}$$

where $\sigma_k \equiv x_k^4 + y_k^4 + z_k^4$ refers to the direction cosines made by $\vec{R}_k$ and σ to those made by $\vec{H}$ with the crystallographic axes.

We have generated, by computer, the crystal lattice of lead and calculated the expressions $d^6\sum_i S_i$ for the different shells (d is the lattice constant). We show in Table I the results for the first seven shells.

We note that $d^6\sum_i S_i$ for all shells is of the form $s = p(\sigma - |q|)$ with p positive for some shells and negative for others. For instance, shell Nos. 1, 3, 4, and 7 have the same symmetry characterized by $s_1 = -|p_1|(\sigma - 1.67)$, whereas the second shell is characterized by $s_2 = |p_2|(\sigma - 0.33)$. It is important to realize that the different symmetries cannot be changed by the factors $(1+B_k)^2$, which are always positive.

In the (110) plane, $\sigma = \frac{1}{2}\sin^4\psi + \cos^4\psi$, and $-(\sigma - 1.67)$ and $(\sigma - 0.33)$ have the form shown in Fig. 5. Comparing the dependence of s_1 and s_2 on ψ with that of M_2 given in Fig. 3, we see immediately that the second shell cannot make the major contribution to the second moment. Further, as can be seen from Fig. 3, the experimental anisotropy is very pronounced. If one were to fit the curve to the expression (2) without knowing the theoretical expressions appearing in Table I, one would have to pick $1 < Q < 1.67$. However, contributions from shell Nos. 2 and 5 tend to make $Q < 1.67$. Therefore, unless shell 6 happens to make a large contribution to M_2, which is very unlikely, our experimental results force us to pick $Q = 1.67$. This result indicates that $(1+B_2)^2 \approx 0$, i. e., the atoms of shell 2 contribute at most slightly to the pseudodipolar interaction. A detailed theoretical calcula-

TABLE I. Results of computer calculation of $d^6\sum_i S_i$ for first seven shells.

Shell	$d^6\sum_i S_i$
1	$-90(\sigma - 1.67)$
2	$22.5(\sigma - 0.33)$
3	$-6.67(\sigma - 1.67)$
4	$-1.41(\sigma - 1.67)$
5	$3.17(\sigma - 0.115)$
6	$-0.74(\sigma - 1)$
7	$-1.05(\sigma - 1.67)$

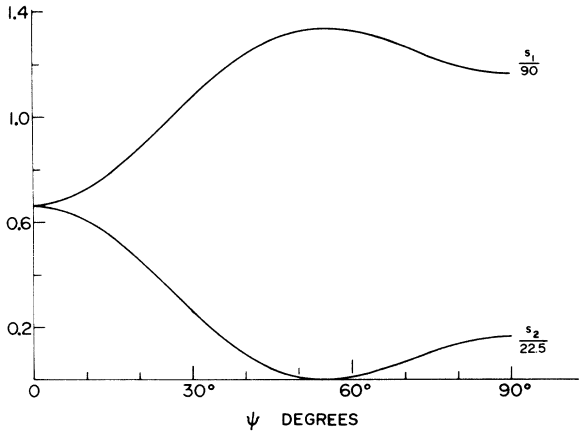

FIG. 5. Theoretical angular dependence of s_1 and s_2 as defined in the text.

tion of b_{ij} would be able to show whether this is due to the fact that $b_{ij}(|\vec{R}_{ij}|)$ happens to have a node at the distance of the second-shell atoms, or whether $b_{ij}(R_{ij}) \approx 0$ due to the symmetry details of the Fermi surface.

If we now make the simplifying assumption that only the first four shells contribute to M_2, and $B_1 = B_3 = B_4 = B$, then we obtain from Eq. (6)

$$M_2 = -\tfrac{3}{5}\gamma^4\hbar^2 I(I+1) f\, d^{-6}(1+B)^2[98.1(\sigma - 1.67)] \times\left(\frac{10^{-6}}{(2\pi)^2}\right) \text{kHz}^2 .$$

The fitted experimental curve is given by $M_2 = -4.1 \times (\sigma - 1.67)$ kHz^2 and shown in Fig. 3. Taking $\gamma = 5.59\times10^3$ rad sec^{-1}G^{-1}, $d = 4.90$ Å at 1 K, $f = 0.21$, $I = \frac{1}{2}$, we obtain $(1+B)^2 = 2.23\times10^2$, then $B = 13.9$ or -15.9. We pick the positive value in keeping with the theoretical calculations of Ref. 10. This yields

$$\frac{b_{01}}{2\pi} = \frac{\gamma^2\hbar 2^{3/2}}{2\pi d^3} B = 1.75 \text{ kHz} ,$$

in fair agreement with the theoretical value of $b_{01}/2\pi = 1.48$ kHz obtained in Ref. 10.

Combining this result, which is now free from the Anderson-Weiss-model assumption, with the spin-echo result (3), we obtain for the Ruderman-Kittel coupling constant the value

$$\frac{J_1}{2\pi} = \frac{1}{\tau_m} - \frac{\gamma^2\hbar 2^{3/2}}{2\pi d^3}(1+B) = 4.64 \text{ kHz} .$$

The theoretical value obtained in Ref. 10 is $J_1/2\pi = 4.81$ kHz.

We note that $J/b = 2.6$. The Anderson-Weiss model[8] requires $J/b \gg 1$. The fact that our lines are Lorentzian in the center, but do not show the proportionality between linewidth and second moment in an angular-dependence study, seems to indicate that the above condition has to be more stringently satisfied if the proportionality is to be assumed. Kittel and Abrahams[21] have shown that resonance lines of magnetically dilute crystals also have a cutoff Lorentzian shape. The 21% dilution in the case of lead does not seem to be low enough to explain the experimental Lorentzian lines; it may, however, be possible that it did somewhat contribute to the effect.

B. Anisotropic Knight Shift

Boon[13] has shown that when spin-orbit coupling is taken into account, the general expression for the anisotropic Knight shift is of the form

$$K_{\text{an}} = \int \frac{d^3r}{r^3}\left[F_{zz}(\vec{r})\,P_2^0(\cos\theta) + O_x(\vec{r})\,P_2^1(\cos\theta)\sin\phi - O_y(\vec{r})\,P_2^1(\cos\theta)\cos\phi\right] . \quad (7)$$

$P_l^m(\cos\theta)$ are the associated Legendre polynomials. $F_{ij}(\vec{r})$ $(i, j = x, y, z)$ is a symmetric-tensor field invariant under the symmetry operations of the crystal and represents the effect on the electron-spin alignment of the orbital motion of the electrons through the anisotropic g factor. $O_i(\vec{r})$ is a pseudovector field also invariant under the symmetry operations of the crystal and is due to cross terms of the conduction-electron nuclear-dipolar interaction and the spin-orbit coupling. The vector $\vec{r}(r, \theta, \phi)$ describes the electron position in the laboratory frame whose z axis is parallel to the magnetic field. The integral is over all space.

Using the character tables[22] for the cubic groups, we find that the pseudovectors O_i form a three-dimensional basis for the irreducible representation T_1, whereas $P_2^1(\cos\theta)\sin\phi \sim zy$ and $P_2^1(\cos\theta)\times\cos\phi \sim zx$ belong to the three-dimensional basis for T_2. The last two terms in the integral are therefore zero in cubic symmetry. The symmetric tensor is given by the following expression[13]:

$$F_{ij}(\vec{r}) = g\mu_B^2 \sum_p g_{ij}(p)\,\frac{\partial f}{\partial\epsilon}\,|\psi_p(r)|^2 ,$$

$$g_{ij} = g\delta_{ij}\sum_{p'\neq p} \times\frac{\langle p|L_i|p'\rangle\langle p'|N_j|p\rangle + \langle p|N_i|p'\rangle\langle p'|L_j|p\rangle}{\epsilon_p - \epsilon_{p'}} , \quad (8)$$

where g is the free-electron g factor, μ_B is the Bohr magneton, $f(\epsilon)$ is the Fermi distribution function, $\psi_p(\vec{r}) \equiv |p\rangle$ are the eigenfunctions of the unperturbed Hamiltonian $p^2/2m + V(\vec{r})$, $\vec{L}$ is the orbital-angular-momentum operator, and $\vec{N} = (h/2m^2c^2)(\nabla V(\vec{r})\times\vec{p})$. The detailed perturbation procedure leading to this result can be found in Ref. 13.

Let us write

$$F_{zz} \equiv \tfrac{1}{3}(3F_{zz} - \text{Tr}F) + \tfrac{1}{3}\text{Tr}F .$$

Since F_{ij} is invariant under the symmetry operations of the crystal, we conclude that the first term transforms as $3z^2 - r^2 \sim P_2^0(\cos\theta)$, whereas the second term forms a basis for the identity representation of the group. Since the latter is multiplied by $P_2^0(\cos\theta)$, which belongs to a basis for the irreducible representation E, its contribution to the integral must vanish, and we are left with

$$K_{an} = \frac{1}{3}\int \frac{d^3r}{r^3}\,[3F_{zz}(r) - \mathrm{Tr}F]\,P_2^0(\cos\theta)\,.$$

Let us define $A(\vec{r})$ by

$$\tfrac{1}{3}[3F_{zz}(r) - \mathrm{Tr}F] = A(\vec{r})\,P_2^0(\cos\theta)\,. \tag{9}$$

$A(\vec{r})$ will then transform according to the identity representation and the anisotropic Knight shift becomes

$$K_{an} = \frac{4\pi}{5}\left(\frac{d^3r}{r^3}\right)A(\vec{r})\,[Y_2^0(\theta,\phi)]^2\,,$$

where Y_l^m are the spherical harmonics. To determine the explicit angular dependence of this expression we will make use of the lattice harmonics in cubic symmetry used by O'Reilly and Tsang[16] in their second-moment calculation.

Using the coupling rule for spherical harmonics and the spherical-harmonic addition theorem we can write

$$Y_2^0(\theta)\,Y_2^0(\theta) = \frac{5}{(4\pi)^{1/2}}\sum_{L=0,2,4}\frac{[C(22L,00)]^2}{(2L+1)^{1/2}}\,Y_L^0(\theta)$$

$$= 5(4\pi)^{1/2}\sum_{L=0,2,4}\sum_{M=-L}^{L}\frac{[C(22L,00)]^2}{2L+1}$$

$$\times Y_L^{M*}(\theta',\phi')\,Y_L^M(\theta,\Phi)\,,$$

where θ', ϕ' are the polar angles of $\vec{r}$, θ, Φ are those of $\vec{H}$ with respect to the crystallographic axes, and $C(22L, 00)$ is a Clebsch-Gordan coefficient. Expanding the spherical harmonics in terms of lattice harmonics, we obtain

$$K_{an} = (4\pi)^{3/2}\sum_{L,\mu,\alpha,i}\frac{[C(22L,00)]^2}{2L+1}$$

$$\times\int \frac{d^3r}{r'^3}\,A'(r')\,X_L^{\mu\alpha i}(\theta',\phi')\,X_L^{\mu\alpha i}(\theta,\Phi)\,,$$

where μ labels the representation, α labels different sets of functions belonging to the same representation, and i labels the different basis functions within a representation. Since $A'(r')$ belongs to the identity, only those lattice harmonics which form a basis for the identity representation of the cubic group will survive in the sum. Since this basis is one dimensional, the sum over i has one term only, and we are left with (call $\mu = 1$ the identity representation)

$$K_{an} = (4\pi)^{3/2}\sum_{L,\alpha}[C(22L,00)]^2\,X_L^{1\alpha}(\theta,\Phi)$$

$$\times\int \frac{d^3r'}{r'^3}\,A'(r')\,X_L^{1\alpha*}(\theta',\phi')\,.$$

The identity-representation lattice harmonics in cubic symmetry are given in Ref. 16: For $L \le 4$ there are only two of them:

$$X_0^1 = \frac{1}{(4\pi)^{1/2}}\,,\quad X_4^1 = \frac{525^{1/2}}{64\pi}\,(\bar{x}^4 + \bar{y}^4 + \bar{z}^4 - \tfrac{3}{5})\,,$$

where $\bar{x}$, $\bar{y}$, $\bar{z}$, are the direction cosines. Denoting

$$C = \frac{1}{4\pi}\int\frac{d^3r'}{r'^3}\,A'(r') \quad\text{and}\quad D = \int\frac{d^3r'}{r'^3}\,A'(\vec{r}')\,X_4^1(\theta',\phi')\,, \tag{10}$$

we obtain $K_{an} = (4\pi/5)\,C + 2\pi(\tfrac{3}{7})^{1/2}D(x^4 + y^4 + z^4 - \tfrac{3}{5})$, where $\bar{x}$, $\bar{y}$, $\bar{z}$ are now the direction cosines made by the magnetic field with the principal axes of the crystal. C is isotropic and therefore cannot be determined experimentally by an angular-dependence study. We incorporate it in K_{iso} and write $K = K_{iso} + 2\pi(\tfrac{3}{7})^{1/2}D(x^4 + y^4 + z^4 - \tfrac{3}{5})$. The average over all space of the second term is zero, as it should be. The angular dependence is completely determined by the above expression.

If we denote again by ψ the angle made by the field with the [001] axis in the (110) plane, we have

$$K = K_{iso} + 2\pi(\tfrac{3}{7})^{1/2}D(\tfrac{1}{2}\sin^4\psi + \cos^4\psi - \tfrac{3}{5})\,.$$

Our experimental result can be written in the form $K = K_{iso} + (0.285/\nu_r)(\tfrac{1}{2}\sin^4\psi + \cos^4\psi - 0.6)$, where ν_r is the resonance frequency of the reference compound. Picking[23] $\nu_r = 8.90772 \pm 4$ MHz, we obtain $K_{iso} = 1.085\%$ and $D = 7.8\times10^{-6}$.

Since the electron eigenfunctions as well as the Fermi surface of lead are fairly well known, D could be calculated from the expressions (8)–(10).

V. CONCLUSION

Our study of the nuclear magnetic resonance in single-crystal lead has shown that the "exchange-narrowing" model of Anderson and Weiss is inapplicable. Further, we have established that the contribution of the second-nearest neighbor to the second moment is very small and we have obtained values for both pseudoexchange and pseudodipolar coefficients for the first-nearest neighbor. A small anisotropy of the Knight shift has been detected for the first time in a cubic metal and it is hoped to pursue this measurement in higher fields and also in purer samples, where it is expected that de Haas–van Alphen–type oscillations in the Knight shift may also occur.

†Research supported by the National Research Council of Canada through Grant No. A-1873.

*H. R. McMillan Predoctorate Fellow.

[1] J. H. Van Vleck, Phys. Rev. 74, 1168 (1948).

[2] M. A. Ruderman and C. Kittel, Phys. Rev. 96, 99 (1954).

[3]N. Bloembergen and T. J. Rowland, Phys. Rev. 97, 1679 (1955).
[4]R. J. Snodgrass and L. H. Bennett, Phys. Rev. 132, 1465 (1963).
[5]H. Alloul and C. Froidevaux, Phys. Rev. 163, 324 (1967).
[6]H. Alloul and R. Deltour, Phys. Rev. 183, 414 (1969).
[7]P. W. Anderson and P. R. Weiss, Rev. Mod. Phys. 25, 269 (1953).
[8]P. W. Anderson, J. Phys. Soc. Japan 9, 316 (1954).
[9]S. N. Sharma, D. Ll. Williams, and H. E. Schone, Phys. Rev. 188, 662 (1969).
[10]L. Tterlikkis, S. D. Mahanti, and T. P. Das, Phys. Rev. Letters 21, 1796 (1968).
[11]C. H. Townes and W. D. Knight, Phys. Rev. 77, 852 (1950).
[12]A. Abragam, *Principles of Nuclear Magnetism* (Oxford U.P., London, 1961).
[13]M. H. Boon, Physica 30, 1326 (1964).
[14]A. C. Chapman, P. Rhodes, and E. F. W. Seymour, Proc. Phys. Soc. (London) 70B, 345 (1957).
[15]H. Wahlquist, J. Chem. Phys. 35, 1708 (1961).
[16]D. E. O'Reilly and T. Tsang, Phys. Rev. 128, 2639 (1962).
[17]E. R. Andrew, Phys. Rev. 91, 425 (1953).
[18]S. D. Mahanti and T. P. Das, Phys. Rev. 170, 426 (1968); L. Tterlikkis, S. D. Mahanti, and T. P. Das, *ibid.* 178, 630 (1969).
[19]J. R. Anderson and A. V. Gold, Phys. Rev. 139, 1459 (1965).
[20]H. Alloul and C. Froidevaux, Colloq. Ampere 14, 457 (1966).
[21]C. Kittel and A. Abrahams, Phys. Rev. 90, 238 (1953).
[22]V. Heine, *Group Theory in Quantum Mechanics* (Pergamon, London, 1960).
[23]E. B. Baker, J. Chem. Phys. 26, 960 (1957).

PHYSICAL REVIEW B VOLUME 5, NUMBER 11 1 JUNE 1972

Effect of Primary-Electron Diffusion on Secondary-Electron Emission

Alan J. Bennett and Laura M. Roth
General Electric Research and Development Center, Schenectady, New York 12301
(Received 3 November 1971)

We consider some effects of primary-electron diffusion on secondary-electron emission from a free-electron model of a polycrystalline target—in particular the angular distribution and energy dependence of the secondaries. The distributions of primary electrons due to incident 2- and 10-keV monoenergetic beams are obtained by means of a Boltzmann equation. The fraction of back-scattered primaries is found to be in good agreement with experiment. The primary distributions excite distributions of secondary electrons which diffuse toward and are transmitted through the surface. In accord with experiment the large angular ansiotropy in the emitted secondary-electron distribution predicted by Stoltz is found to be greatly reduced by the primary diffusion. The transmission coefficient, not included in previous calculations, is also of importance in determining the characteristics of the observed secondaries.

I. INTRODUCTION

The problem of secondary-electron emission[1-3] has received renewed interest recently in part due to the development of the scanning electron microscope. An extensive review of the previous work on this complete subject has been given by Hachenberg and Brauer.[1] Briefly, when a target is bombarded with primary electrons of a given energy and direction relative to the surface normal, secondary electrons (< 50 eV) are emitted with a current distribution $j_s^0(E, \Omega)$, which is a function of secondary energy E and direction Ω. Due to the difficulty of the measurements, most experiments yield information about various integrals of $j_s^0(E, \Omega)$. These are the pure angular distribution $j_s^0(\Omega) = \int j_s^0(E, \Omega) dE$, the pure energy distribution $j_s^0(E) = \int j_s(E, \Omega) d\Omega$, and the yield $= \int\int j_s^0(E, \Omega) dE\, d\Omega$.

Jonker[4] measured $j_s^0(E, \Omega)$ for primaries normally incident on polycrystalline Ni and found that the angular distribution of the secondary current obeyed a cosine law characteristic of an isotropic distribution of secondaries inside the material. On the other hand, theoretical calculations primarily due to Stoltz[5] predicted an angular distribution which is considerably flattened.

We consider in this paper the effect of primary-electron diffusion on secondary-electron emission, in particular, on the angular distribution and energy dependence of secondaries when the primary energy is 2 and 10 keV. The latter primary energy is characteristic of scanning-electron-microscope operation. One aim of this work is to resolve the above-mentioned discrepancy regarding the angular dependence. Another aim is to calculate the pure energy distribution as a function of primary direction and energy. Experimentally, the yield is found to increase with increasing primary energy up to about 500 eV and then to decrease. For a fixed primary energy the yield increases as the primary beam deviates from normal incidence. This is often attributed to the